



All-optical spin injection in silicon investigated by element-specific time-resolved Kerr effect: supplement

SIMONE LATERZA,^{1,2,*}  ANTONIO CARETTA,^{1,7} RICHA BHARDWAJ,¹ ROBERTO FLAMMINI,³ PAOLO MORAS,⁴ MATTEO JUGOVAC,⁴ PIU RAJAK,⁵ MAHABUL ISLAM,⁵ REGINA CIANCIO,⁵ VALENTINA BONANNI,¹ BARBARA CASARIN,² ALBERTO SIMONCIG,¹ MARCO ZANGRANDO,^{1,5} PRIMOŽ REBERNIK RIBIČ,¹ GIUSEPPE PENCO,¹ GIOVANNI DE NINNO,¹ LUCA GIANNESI,¹  ALEXANDER DEMIDOVICH,¹ MILTCHO DANAILOV,¹ FULVIO PARMIGIANI,^{1,6} AND MARCO MALVESTUTO^{1,5}

¹*Elettra Sincrotrone Trieste, S.C.p.A. Strada Statale 14-km 163.5 in AREA Science Park 34149 Basovizza, Trieste, Italy*

²*Department of Physics, University of Trieste, Via A. Valerio 2, 34127 Trieste, Italy*

³*Istituto di Struttura della Materia-CNR (ISM-CNR), Via del Fosso del Cavaliere 100, 00133, Roma, Italy*

⁴*Istituto di Struttura della Materia-CNR (ISM-CNR), SS 14 km 163.5, I-34149, Trieste, Italy*

⁵*Istituto Officina dei Materiali (CNR-IOM), SS 14 km 163.5, I-34149, Trieste, Italy*

⁶*International Faculty, University of Cologne, 50937 Cologne, Germany*

⁷*e-mail: antonio.caretta@elettra.eu*

**Corresponding author: simone.laterza@elettra.eu*

This supplement published with Optica Publishing Group on 28 November 2022 by The Authors under the terms of the [Creative Commons Attribution 4.0 License](https://creativecommons.org/licenses/by/4.0/) in the format provided by the authors and unedited. Further distribution of this work must maintain attribution to the author(s) and the published article's title, journal citation, and DOI.

Supplement DOI: <https://doi.org/10.6084/m9.figshare.21179458>

Parent Article DOI: <https://doi.org/10.1364/OPTICA.471951>

All-optical spin injection in silicon investigated by element specific time-resolved Kerr effect: supplemental document

Section I. Sample synthesis and characterization.

The sample was prepared and characterized under ultra-high vacuum conditions at the end-station of the VUV-Photoemission beamline (Elettra Sincrotrone Trieste). The Si substrate was cut from a p-doped Si wafer (B dopant, 0.05 Ωcm resistivity) with (111) surface termination. After prolonged thermal annealing at 700 K, the substrate was flash-annealed to 1520 K until a sharp 7×7 surface reconstruction appears in the low-energy electron diffraction (LEED) pattern. The topmost photoemission spectrum in Fig. S1 (black line) refers to this preparation step. The surface was held at a temperature of 1050 K and exposed to 100 L of NH_3 to produce an ultra-thin layer of crystalline $\text{Si}_3\text{N}_4(0001)$. This reaction is known to be self-limiting at the thickness corresponding to two bilayers (< 1 nm), which display an 8×8 surface reconstruction in the LEED pattern [1]. The formation of the Si_3N_4 layer is accompanied by the presence of the $\text{N}1s$ level and the shifted components in the $\text{Si}2p$ and $\text{Si}2s$ levels (red spectrum in Fig. 1S). Ni was grown on the $\text{Si}_3\text{N}_4(0001)$ surface kept at liquid nitrogen temperature, to favor the formation of a continuous film. As shown in Fig. S1 (green spectrum), the Ni film thickness of 7 nm is sufficient to suppress almost completely the signal from the $\text{Si}_3\text{N}_4(0001)$. The Ni film displays no LEED pattern. Finally, an Ag film of 2 nm was deposited on Ni, again using liquid nitrogen temperature to obtain a uniform coverage (blue spectrum of Fig. S1). This was particularly important to prevent the oxidation of Ni, as the sample was removed from the growth chamber for the magnetic measurements.

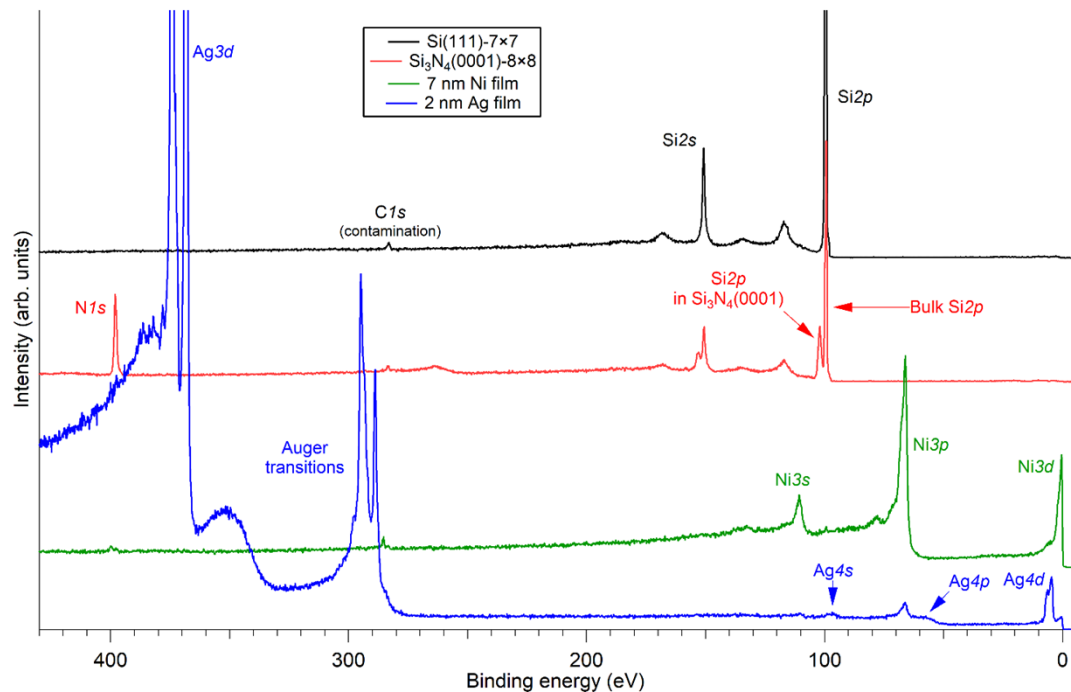


Fig. S1: Photoemission spectra taken at the various stages of the sample growth.

Section II. TEM characterization of the sample.

Details on the film nanostructure were provided by high-resolution transmission electron microscopy (HRTEM) using a JEOL 2010 UHR field emission gun microscope operated at 200 kV with a measured spherical aberration coefficient C_s of 0.47 ± 0.01 . A representative bright-field HRTEM image of the Ni/ Si_3N_4 /Si(111) cross-section is shown in Fig. S2. The Si_3N_4 layer is about 0.7 nm-thick and homogeneously extends on top of the bare Si (111) substrate with atomically flat and sharp interfaces. In the close proximity of Si_3N_4 interface in the semiconductor, a limited interdiffusion of Ni atoms can give rise to a nickel silicide layer with a calculated stoichiometry corresponding to NiSi_2 . The silicide layer was not uniform in all the probed regions of the sample, but its thickness was always observed to be below 3 nm.

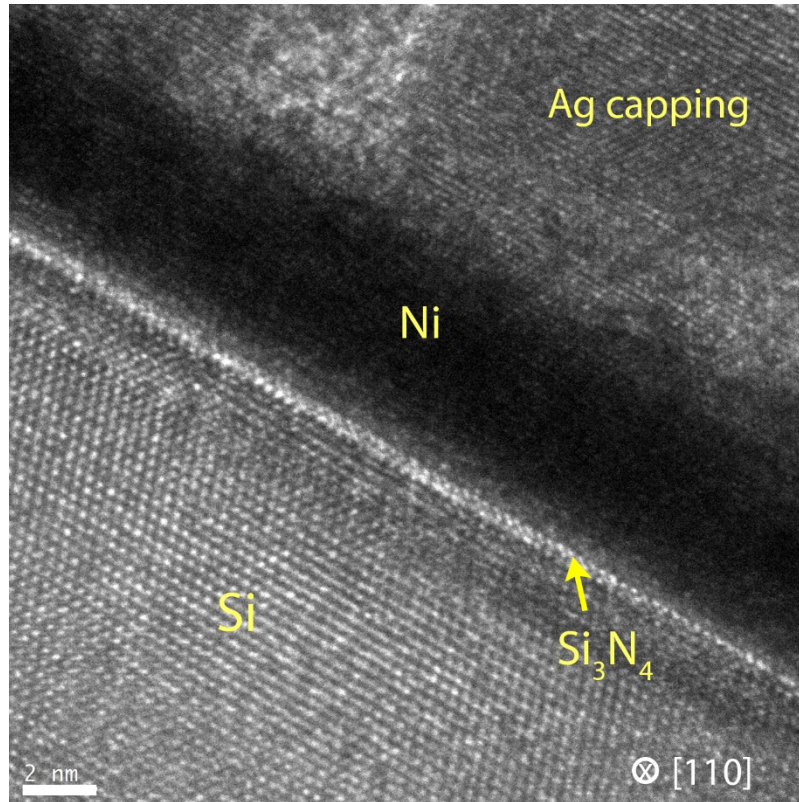


Fig. S2: Cross-sectional HRTEM image of Ni/ Si_3N_4 /Si (111) nanostructure.

Section III. Kerr rotation calculation

Fig. S3 displays the calculated Kerr rotation for bulk Ni sample.

Calculation procedure: First, the real components of the dielectric tensor for Ni have been calculated with DFT package WIEN2k [2] and then extended to the imaginary parts using the Kramers-Kronig relations, making sure that they converged to zero at higher energies. Then using the magneto-optical medium boundary matrix formation [3, 4], the Kerr rotation in longitudinal geometry at 45° angle of incidence was calculated. In the Figure S3, we have highlighted the Ni $M_{2,3}$ (red) and Si $L_{2,3}$ (blue) edge. The calculations further support the fact that no magneto-optical effect arising from Ni M-edge is present at the Si L-edge.

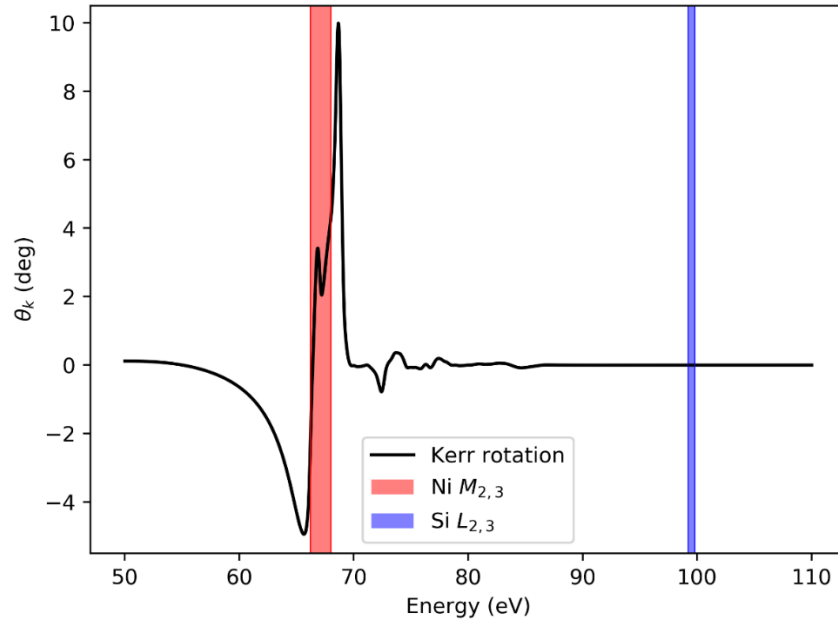


Fig. S3: Kerr rotation for a bulk Ni sample.

References

1. R. Flammini, P. Allegrini, F. Wiame, R. Belkhou, F. Ronci, S. Colonna, D. M. Trucchi, F. Filippone, S. K. Mahatha, P. M. Sheverdyeva, and P. Moras, *Phys. Rev. B* 91, 0075303 (2015). This corresponds to Ref. 24 of the main text.
2. P. Blaha, K. Schwarz, F. Tran, R. Laskowski, G. K. H. Madsen, and L. D. Marks, *J. Chem. Phys.* 152, 074101 (2020)
3. T. Yoshino, and S. Tanaka, *Jpn. J. of Appl. Phys.* 5, 989 (1966).
4. J. Zak, E. R. Moog, C. Liu, and S. D. Bader, *Phys. Rev. B* 43, 6423 (1991)